Available online at www.sciencedirect.com
ScienceDirect
Planetary and Space Science 55 (2007) 280–288
Planetary and Space Science
www.elsevier.com/locate/pss

Lithospheric structure in the eastern region of Mars' dichotomy boundary

Colleen A.E. Milbury[a,*], Suzanne E. Smrekar[b], Carol A. Raymond[b], Gerald Schubert[a,c]

[a]Department of Earth and Space Sciences, University of California, Los Angeles, CA, USA
[b]Jet Propulsion Laboratory, California Institute of Technology, Pasadena, CA, USA
[c]Institute of Geophysics and Planetary Physics, University of California, Los Angeles, CA, USA

Accepted 7 March 2006
Available online 22 August 2006

Abstract

We examine gravity, topography, and magnetic field data along the well-preserved Martian dichotomy boundary between 105° and 180°E to better understand the origin and modification of the dichotomy boundary. Admittance modeling indicates bottom-loading for the Amenthes region (105–135°E) with crustal and elastic thickness estimates of 15–40 km, and 15–35 km and top-loading for the Aeolis region (145–180°E) with crustal and elastic thickness estimates of 10–20 km and 10–15 km, respectively. There is a general trend from bottom-loading in the west, to top-loading in the east. The bottom-loading signature near Amenthes may reflect its proximity to the Isidis basin or a broad valley southeast of Isidis. Surface volcanic deposits may produce the top-loading seen at Aeolis. Additional processes such as erosion and faulting have clearly affected the dichotomy and may contribute to the loading signature. Low elastic thickness estimates are consistent with loading in the Noachian, when heat flow was high. Significant Bouguer and isostatic gravity anomalies in these areas indicate substantial variations in the crustal density structure. Crater age dating indicates that major surface modification occurred early in the Noachian, and the small elastic thickness estimates also suggest that subsurface modification occurred in the Noachian. Magnetic and gravity anomalies show comparable spatial scales (several hundred kilometers). The similarity in scale and the constant ratio of the amplitudes of the isostatic and Bouguer gravity to the magnetic anomalies along the dichotomy suggest a common origin for the anomalies. Igneous intrusion and/or local thinning or thickening of the crust, possibly with a contribution from hydrothermal alteration, are the most likely mechanisms to create the observed anomalies.

Keywords: Mars; Dichotomy; Gravity; Isostasy; Crustal magnetism

1. Introduction

Mars' global dichotomy boundary separates the relatively smooth northern lowlands from the heavily cratered southern highlands. It is a fundamental feature of the planet, yet its origin is not well understood. Studies have proposed endogenic and exogenic models as mechanisms for dichotomy formation. Endogenic models include thinning or thickening of the crust and/or lithosphere above a degree 1 mantle convection pattern (Schubert and Lingenfelter, 1973; Wise et al., 1979a, b; Breuer et al., 1997, 1998; Zhong and Zuber, 2001) and resurfacing due to plate tectonics (Sleep, 1994). Exogenic models include single (Wilhelms and Squyres, 1984) or multiple (Frey and Schultz, 1988) impact events.

This study focuses on the relatively well-preserved region of the dichotomy boundary from 105° to 180°E. This region has not been affected by major impact basins or volcanic centers. Unlike the Arabia Terra section of the dichotomy, the slope between the highland–lowland transition is relatively high and the increase in crustal thickness is rapid (Zuber et al., 2000; Neumann et al., 2004). We seek to understand the compensation mechanisms and lithospheric structure in this region, as well as the nature of the magnetized crust. Ultimately, the goal is to understand the origin of the dichotomy boundary and its subsequent modification. We compare our results

*Corresponding author. Tel.: +1 310 825 3118; fax: +1 310 825 2779.
E-mail address: cmilbury@ess.ucla.edu (C.A.E. Milbury).

0032-0633/$ - see front matter © 2006 Elsevier Ltd. All rights reserved.
doi:10.1016/j.pss.2006.03.009

with a similar study of the Ismenius region (Smrekar et al., 2004).

The study area is divided into two parts, which we call Amenthes (105–135°E, 15°S–15°N) and Aeolis (145–180°E, 25°S–5°N), based on nearby mapping quadrangles (Fig. 1). The boundaries were chosen in an attempt to avoid the gravity signatures of Elysium Mons and the Isidis impact basin. The transition in the crustal thickness in both areas parallels the topography.

2. Data

Free-air gravity and topography data used are specified on 1° Cartesian grids derived from the spherical harmonic gravity model MGS95I (an update of Yuan et al. (2001), carried out to degree and order 95) computed to degree and order 50, and the MOLA topography, respectively. The J_2 term has been removed. The gravity and topography are calculated with respect to the center of mass using a reference radius of 3397 km. Fields computed to degree and order 70 were also examined, but appeared, at least locally, to contain artifacts. We model the gravity and topography data out to a relatively conservative degree and order of 50 to prevent over-interpretation of the data. The degree strength of the gravity field is the degree at which the noise and signal in the power spectra have approximately equal amplitudes. The spacecraft altitude and local degree strength are approximately 400 and 425 km (degrees and order 50), respectively, although the data are downward continued to the surface. We use values of 2900 kg/m^3, 3500 kg/m^3, 9×10^{10} Pa, and 0.25 for crustal density, mantle density, Young's modulus, and Poisson's ratio, respectively. The magnetic field model we consider is the equivalent point source inversion of Langlais et al. (2004). Langlais et al. (2004) use both AeroBraking (AB) and nighttime Science Phase Orbit (SPO) (~150 km orbital altitude) and Mapping Orbit (MO) (~400 km orbital altitude) data in their inversion. The magnetic anomaly fields have been calculated at an altitude of 160 km. The resolution of the magnetic field data is inherently higher than the gravity data due to the incorporation of magnetic data from the low-altitude AB phase.

3. Methods

The admittance method examines the relationship between gravity and topography in the spectral domain, and is sensitive to the elastic thickness of lithosphere

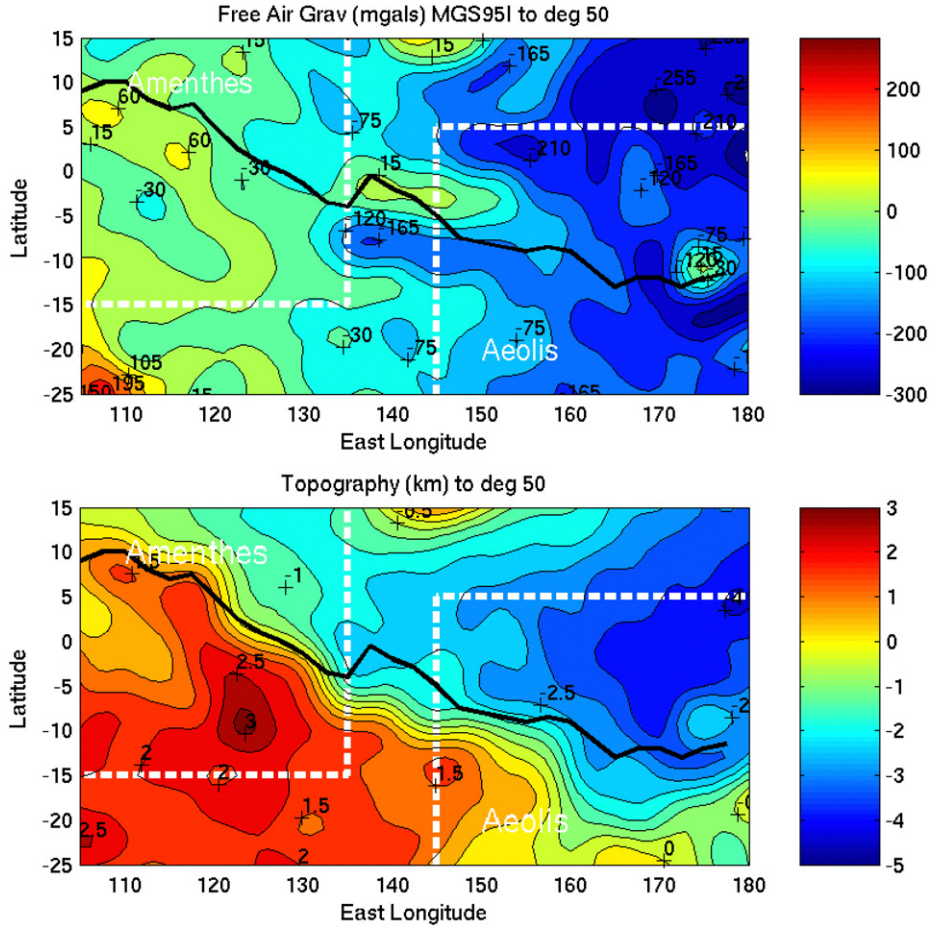

Fig. 1. Free-air gravity anomalies (top), and topography (bottom). The black curve is the dichotomy boundary, and the dashed white boxes indicate the study areas.

because the elastic thickness controls the response of the surface to loads of a given size. Compensation occurs via isostatic, elastic, or dynamic processes. In general dynamic processes are not relevant for Mars because of its geologic inactivity. Admittance $Q(k)$ is the ratio of gravity to topography and is defined as the transfer function between the spectral representation of the gravity $G(k)$ and topography $H(k)$ (Dorman and Lewis, 1970) and assumes that the lithosphere is laterally isotropic:

$$G(k) = Q(k) * H(k) + N(k),$$

where $k = \sqrt{k_x^2 + k_y^2}$ is the two-dimensional wavenumber $2\pi/l$ and l is the wavelength (Dorman and Lewis, 1970; Forsyth, 1985). $N(k)$ is the noise in the data, which is assumed to be small. In the Cartesian approach, the data are averaged over discrete wave number bands to prevent bias by noise. The admittance estimate is written as

$$Q(k) = \frac{\langle GH^* \rangle}{\langle HH^* \rangle},$$

with angle brackets indicating averaging over wave number bands and the asterisk denotes the complex conjugate. The ratio of the gravity and topography changes depending on whether the topography is supported by the strength of the elastic lithosphere, or by variations in subsurface density, such as crustal thickness changes. Flexural compensation assumes that loads are partially supported by stresses within the elastic lithosphere, and partially by deflection of the lithosphere overlying a fluid asthenosphere. The relative importance of isostasy versus flexure in compensating loads at a given wavelength depends on the flexural rigidity D of the elastic plate, given by

$$D = \frac{E\,T_e^3}{12(1-\upsilon^2)},$$

where E is the Young's modulus, υ the Poisson's ratio, and T_e the elastic thickness. A large elastic thickness corresponds to a strong lithosphere in which elastic stress supports a significant fraction of loading, and small elastic thickness implies relatively little elastic support of stress.

The standard transfer function for loading of the elastic lithosphere from above was developed by Banks et al. (1977):

$$Q_T(k) = 2\pi\rho_c G\left[\frac{1 - e^{-kZ_C}}{1 + \frac{Dk^4}{g\,\Delta\rho}}\right],$$

where G is the gravitational constant, Z_C the thickness of the crust, and $\Delta\rho = \rho_m - \rho_c$ the density contrast at the crust mantle boundary. For a bottom-loaded region, the short wavelength slope is negative because small loads at depth will produce little surface deformation. An area that is locally compensated by variations in crustal thickness has a constant positive slope in the admittance curve. For bottom-loading the admittance (McNutt, 1983),

$$Q_N(k) = 2\pi G\{\rho_c + (\rho_m - \rho_c)\,e^{-kZ_c} - [(Dk^4 + \rho_m g)/g]\,e^{-kZ_L}\}.$$

This generalized form of the bottom-loading equation includes a second compensation depth Z_L below the crust mantle boundary interface. This depth is typically assumed to represent the density contrast near the base of the thermal lithosphere, such as would be due to a low-density mantle plume pushing up on the lithosphere. As the value of Z_L approaches that of Z_C, the effect of the Z_L term becomes small.

For Cartesian datasets, a variety of different methods are available to minimize aliasing of wavelengths larger than the box size, such as mirroring the data (e.g., McNutt, 1983) or using multitaper methods (Simons et al., 2000; and references therein). The multitaper method has been shown to cause a systematic bias toward low values for high elastic thicknesses ($T_e > 40$ km), but is quite accurate for low elastic thicknesses (Swain and Kirby, 2003). When the Cartesian method is used in this study, the data are mirrored to reduce the effects of windowing the data. We first calculate the observed admittance and then compare it to the admittance predicted, calculated using the topography for each region, and a range of elastic thickness values. Surface and subsurface loads are deconvolved from the data for a given elastic thickness, and admittance spectra are then calculated assuming that the loads are statistically uncorrelated. The best-fit elastic thickness estimate is that which yields a minimum root-mean-square error between the observed and predicted admittance.

3.1. Isostatic and Bouguer anomalies

We calculate Bouguer and isostatic anomalies to examine the spatial variability in the subsurface structure. The Bouguer gravity anomaly removes the effect of topography from the free-air gravity, and the isostatic anomaly removes the effect of an isostatic crustal layer from the Bouguer gravity. We calculate the isostatic anomaly assuming a 50 km thick crustal layer overlying a mantle that is 600 kg/m^3 denser, as well as deviations from a 50 km thick isostatic layer (Fig. 2). Estimates of the average global crustal thickness are consistent with 50 km (see Table 1). Maps of the Bouguer anomalies with superimposed magnetic anomaly field (Langlais et al., 2004) are given in Fig. 3.

4. Results

Both the Amenthes and Aeolis regions show positive and negative isostatic and Bouguer anomalies that straddle the dichotomy boundary, similar to the Ismenius region (Smrekar et al., 2004). The isostatic anomalies show similar patterns. Variations in either the density contrast or the thickness of the crust will change the absolute amplitude of the isostatic anomalies, but not their location or relative amplitudes.

In order to assess the spatial variability of admittance along the dichotomy boundary, we examine 13 gravity and topography windows. These windows are spaced at 5–10°

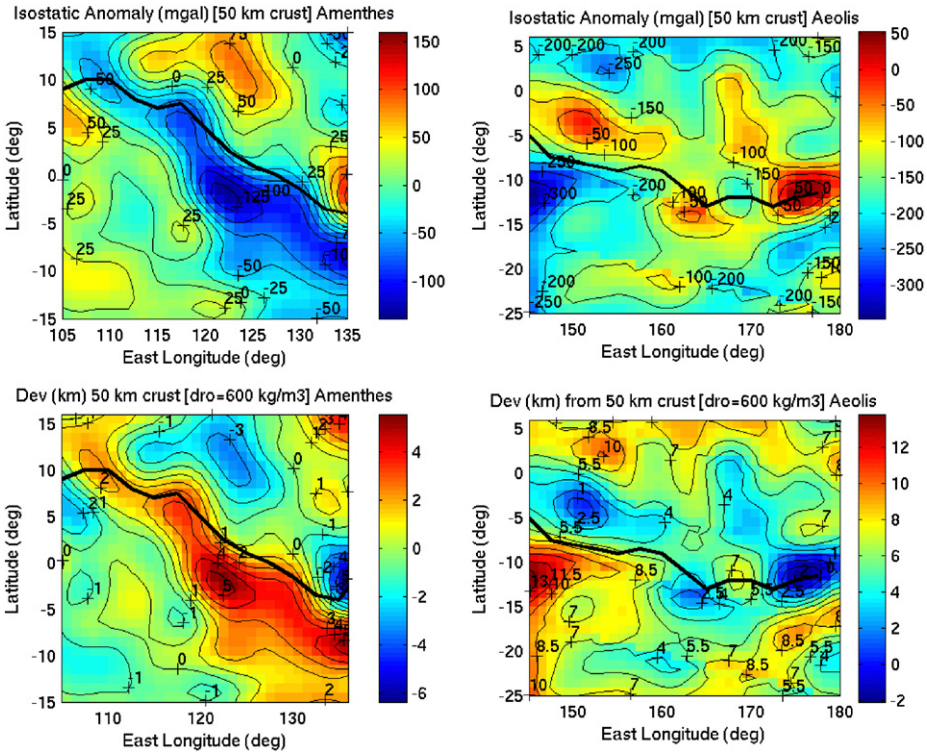

Fig. 2. The isostatic anomaly (in mgal) for Amenthes (top, left) and Aeolis (top, right). Deviations from a 50 km thick crust (in km) for Amenthes (bottom, left) and Aeolis (bottom, right). The dichotomy boundary is the thick black line.

Table 1
Summary of previous results

Reference	Longitude	Latitude	Crustal thickness (km)	Elastic thickness (km)
Zuber et al. (2000)	Global		44	N/A
Turcotte et al. (2002)	Global		90 ± 10	90 ± 10
Neumann et al. (2004)	Global		>45	N/A
Smrekar et al. (2004)	50–90°E	30–60°N	10–30	0–15
Watters (2003)	112–136°E	12°S–12°N	N/A	31–36
Watters and McGovern (2006)	110–160°E	20°S–10°N	N/A	~30
Nimmo (2002)	110–220°E	40°S–20°N	1–75	37–89
Kiefer (2005)	130–155°E	10°S–30°N	40–60	< 25

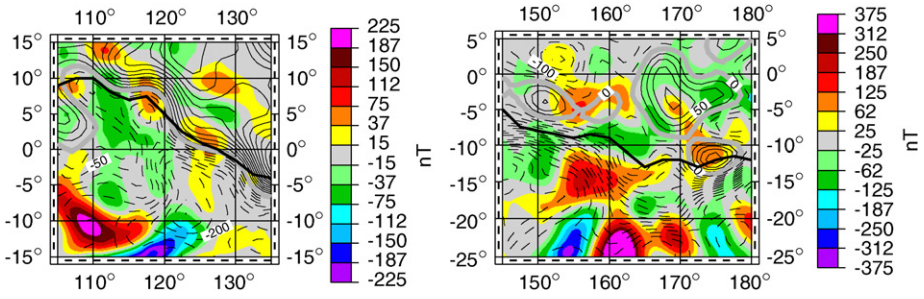

Fig. 3. Bouguer anomaly contours (mgals) for the Amenthes region (left) and the Aeolis region (right), superimposed on the radial component of magnetic field (nT) (Langlais et al., 2004) at an altitude of 160 km in color. Positive Bouguer values are in dashed black lines, negative values are solid black, and 0 is gray. The dichotomy boundary is the thick black line.

latitudinal intervals and range from 50° to 180°E with a minimum box size of $32° \times 32°$. The best-fit crustal and elastic thickness values are 15–40 km and 15–35 km for Amenthes, and 10–20 km and 10–15 km for Aeolis, respectively (Table 2). We find a transition from bottom-loading in the west to top-loading in the east. For Aeolis, the fit error of 2.3 mgal/km for a top-load (Fig. 4, Table 2) is smaller than the fit error of 3.8 mgal/km found using a

Table 2
Crustal and elastic thickness results with rms errors

Region	Crustal thickness (km)	Elastic thickness (km)	Observed error (mgal/km)	Fit error (mgal/km)
Amenthes	15–40	15–35	5.6	4.7
Aeolis	20 (October)	15 (October)	4.4	2.3

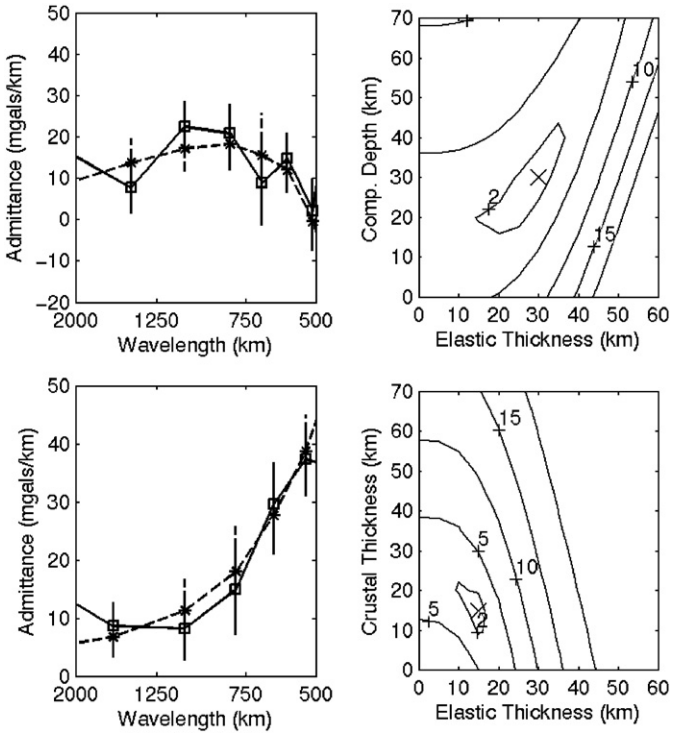

Fig. 4. The observed and predicted admittance with error bars are shown for the Amenthes (top, left) and the Aeolis regions (bottom, left). The observed and predicted admittance is indicated by the solid line with squares and the dashed line with asterisks, respectively. The error analysis is shown for the Amenthes (top, right), and the Aeolis regions (bottom, right). The model with the minimum error is marked by 'X'.

bottom-load. For Amenthes, bottom-loading gives the best fit of 5.6 mgal/km (Table 2); top-loading also gives a reasonable fit error of 6.9 mgal/km. We tested a smaller crust mantle density contrast of 400 kg/m^3, to determine its effect on estimated parameters. The best-fit crustal and elastic thickness estimate was the same, but the error was increased. The bottom-loading signature is present for windows containing a broad valley that extends over 1200 km southeast from Isidis. It is not possible to distinguish whether the bottom-loading is associated with this valley or with Isidis. Isidis has a bottom-loading signature with a much higher amplitude (~100 mgal/km) than Amenthes. Amenthes shows low amplitude admittance, which may be influenced by erosion. Although the volcano Apollinaris Patera is within the region we define as Aeolis, the top-loading signature also extends into regions west of Aeolis that exclude the volcano.

Coherence is the statistical relationship between gravity and topography. We calculated and modeled the coherence for different ratios of the surface to subsurface load. However, the gravity and topography data quality and resolution on Mars is such that coherence cannot be used to constrain the loading mechanism and elastic thickness. In their analysis of admittance spectra for Mars, (McGovern et al., 2002) suggest that correlation values greater than 0.5 imply a viable admittance analysis. The correlation between the gravity and topography for Amenthes and Aeolis ranges from 0.6 to 0.9.

It is important to understand the biases inherent in interpreting gravity and topography data in the absence of ground truth. Numerous studies have investigated the effects of admittance analysis versus coherence analysis, filtering methods, spherical harmonic versus Cartesian geometry, spatial versus spectral analyses (e.g., Forsyth, 1985; McKenzie et al., 2002; Perez-Gussinye et al., 2004; Wieczorek and Simons, 2005; and references therein). In all of these studies, the major differences in results for different approaches occur when the actual elastic thickness estimates are large, which are not relevant to our results. Given inherent uncertainties, we use a relatively generous estimate of error. Additionally, our main objective is to compare estimates of elastic thickness from region to region in a relative sense rather than interpreting specific values in detail. Our limited knowledge of both heat flux and the composition of the Martian crust, and especially the volatile and radiogenic content, similarly introduces uncertainty into extrapolation from elastic thickness to heat flux. We anticipate higher resolution data from the Mars Reconnaissance Orbiter in 2007, perhaps to spherical harmonic degree and order 100, which will make it possible to effectively use coherence and increase our confidence in absolute values of lithospheric parameters.

5. Discussion

Our crustal thickness estimates are somewhat lower than the global averages (Zuber et al., 2000; Neumann et al., 2004), but are comparable to estimates for the average thickness of the northern lowlands. These differences are interesting, but there may not be sufficient information to determine the source of the difference. Alternative methods have different biases, but most likely the variations reflect local compositional variations or a phase transition, such as a gabbro–eclogite phase transition (Babeyko and Zharkov, 2000). The significant isostatic anomalies seen in Amenthes and Aeolis indicate large non-isostatic density variations and are likely to skew estimates of crustal thickness. The estimated values of elastic and crustal thickness for Amenthes and Aeolis overlap within the errors. The somewhat larger values of elastic and crustal thickness found at Amenthes may be a result of the bottom-loading model, which is biased towards larger values (Petit and Ebinger, 2000).

Overall, the amount of bottom-loading is greater for Amenthes, with progressively more top-loading evident to the east, and a clear top-loading signature for Aeolis. The bottom-loading signature in Amenthes may be due to a broad valley within this region, possibly from crustal thinning and inflow of mantle material associated with rifting. It may also be influenced by the proximity of the Isidis impact basin. The bottom-loading could also be a fossil signature of a thermal anomaly associated with Isidis or other thermal processes. Amenthes and Aeolis have different geologic surface units. Amenthes is covered with volcanic and sedimentary materials, while Aeolis is close to the Elysium volcanic province as well as Apollinaris Patera and is covered by lava flows (Tanaka et al., 1992, 2005). These surface flows may be the source of top-loading in Aeolis. Aeolis has more plains coverage in the study region. However, the plains are shown to be dominated by bottom-loading (Hoogenboom and Smrekar, 2006). Thus, a nominal plains' signature is not dominant in the region we have defined as Aeolis. Like Aeolis, the Ismenius region also shows a top-loading signature (Smrekar et al., 2004). The top-loading signature points to a role for near surface processes, such as igneous intrusion, sedimentation, and possible serpentinization. Processes such as crustal thinning or thickening, in some cases associated with major impact craters, or deeper intrusions can produce bottom-loads. It is likely that both top- and bottom-loading processes have affected the entire dichotomy region. Without detailed coherence modeling, we can simply note which signature is dominant. For low values of elastic thickness, the fits to the admittance spectra are not drastically different for the two end member models. Although the different loading histories are intriguing, elastic thickness estimates are small, and isostatic compensation cannot be ruled out.

Our estimates of lithospheric properties for this section of the dichotomy are generally in good agreement with results from other studies (see Table 1). Nimmo (2002) uses admittance to obtain crustal and elastic thickness estimates that are higher than our values, but his study area is considerably broader and may be influenced by the highlands and diverse geologic terrains. In addition, he does not use the windowing applied here. The region Kiefer (2005) studies is primarily a highlands subsection of our Amenthes region. His estimate of elastic thickness of <25 km for this region, obtained using a spatial bottom-loading model, overlaps with our result. His crustal thickness is an assumed rather than derived value. Watters (2003) models lithospheric flexure and estimates an elastic thickness of 31–36 km for a region analogous to Amenthes, consistent with our results within the error bars.

The low values of elastic thickness obtained for both regions are generally consistent with values found for other Noachian age terrains (McGovern et al., 2002; Watters, 2003; Watters and McGovern 2006; Smrekar et al., 2004; Kiefer, 2005), and reflect the high heat flow expected early in Mars' history. Although the dichotomy boundary has clearly undergone modification by numerous processes including erosion, tectonism, cratering, and at least locally, volcanism, all major surface modifications happened in the Noachian to early Hesperian, as indicted by crater counts (Tanaka et al., 1992; McGill and Dimitriou, 1990; Frey, 2006). Major density anomalies along the dichotomy boundary also suggest that subsurface density variations have loaded the lithosphere (Smrekar et al., 2004; Kiefer, 2005). Albert and Phillips (2000) demonstrate that flexural parameters measured at present reflect the lithosphere's mechanical response at the time of loading, i.e., the flexure has been effectively 'frozen-in'. We expect any viscous response would have dissipated in the first 1–2 Myr after loading (Watts and Zhong, 2000). Although it is curious that the elastic and crustal thickness are similar for both Aeolis and Amenthes, as discussed above, our crustal thickness estimates are likely affected by numerous subsurface density anomalies. Although not likely to be a factor early in the history of Mars when heat flow was relatively high, the elastic thickness estimates can also be influenced by a mantle elastic response (Burov and Diament, 1995; Guest and Smrekar, 2005).

Prior studies propose a variety of models to explain the observed gravity anomalies and loading signatures. In addition to estimating elastic thickness and loading history, Smrekar et al. (2004) discuss the correlation of geology, gravity, and magnetic anomalies in the Ismenius region, which is generally not observed for other regions of Mars. For example, in the southern highlands large-scale high amplitude linear magnetic anomalies (Connerney et al., 1999, 2001) do not correlate with gravity anomalies (Zuber et al., 2000). Smrekar et al. (2004) note the similarity in the amplitude and size distribution of the gravity and magnetic field anomalies in the Ismenius region of the dichotomy. Their 2D modeling of the gravity and magnetic anomalies suggests that they may be caused by either correlated or anti-correlated subsurface bodies, where correlated bodies imply that the sources for both gravity and magnetic fields are the same; anti-correlated sources may indicate that the lithosphere was modified by a process that created a density contrast, but erased the crust's magnetism by heating after the dynamo ceased. They propose various mechanisms to explain the pattern of gravity and magnetic anomalies, including igneous intrusions, edge-driven convection, crustal thinning or thickening, and hydrothermal alteration. Detailed modeling of the gravity and magnetic anomalies may provide a means to discriminate among these mechanisms, as will higher resolution data sets.

Prior gravity and flexure studies of the dichotomy have been interpreted to indicate a range of processes that have modified the dichotomy boundary. Watters (2003) and Watters and McGovern (2006) suggest that volcanic loading of the lowlands, sedimentary loading and unloading, and planetary contraction may contribute to flexure of the lithosphere. Watters and McGovern (2006) propose that overturn of a magma ocean could create a broken

plate. Kiefer (2005) advocates localized crustal thinning driven by edge-driven convection, in turn initiated by the thermal structure created by Utopia and Elysium impact basins, as a likely explanation for a large, linear positive gravity anomaly. He infers that igneous intrusion is unlikely based on the lack of volcanic activity observed in this area.

Each of these studies advocates a particular interpretation consistent with their specific analysis. Based on modeling of the gravity and topography alone, none can be eliminated. In fact, it is likely that multiple processes have modified the dichotomy. We find some processes more plausible than others, particularly when the magnetic and gravity anomalies are considered. Amenthes and Aeolis each show local regions of possible correlation between the gravity and magnetic anomalies. Correlated magnetic and gravity anomalies will not necessarily lie in exactly the same location, but may be offset slightly due to differences in the direction of the magnetization of the crust imparted by the direction of the ancient magnetizing field. These correlations are generally more prominent in the northern lowlands portion of the study areas, perhaps due to either greater surface erosion, thinner crust, or both. The observed correlation is stronger for Aeolis, which could be related to the greater coverage of lowlands area for Aeolis than for Amenthes. In Amenthes and Aeolis, higher amplitude gravity and magnetic anomalies are observed than those in Ismenius. The ratio of magnetic anomaly to gravity anomaly amplitude remains roughly constant in each region, although the amplitudes of the anomalies increase considerably with longitude. Aeolis is north of the highly magnetized Terra Cimmeria region, and exhibits the highest amplitude magnetic anomalies of all three regions. The increase in magnetic anomaly amplitude towards the Terra Cimmeria region may indicate a thickening of the source layer; however, the concomitant increase in gravity anomaly amplitude suggests an explanation in terms of geologic processes that modified the crust, affecting both the magnetic and density properties and structure. In all regions, the amplitudes of the magnetic anomalies rapidly decrease northward into the lowlands.

A number of studies suggest that the bulk of the crust, the dichotomy boundary, and the dynamo were all created in the early part of the Noachian (Zuber, 2001; Solomon et al., 2005). The low elastic thickness values suggest that the flexural signature of the dichotomy was determined early in Mars' history. This is consistent with image data showing that the boundary has clearly been modified by processes such as impact cratering, faulting, erosion, and at least locally by volcanism during the Noachian (Phillips et al., 2001; Zuber, 2001; Frey et al., 2002; Frey, 2006; Solomon et al., 2005) when the elastic thickness was likely low. The magnetic and gravity anomalies that extend from the highlands into the lowlands adjacent to the boundary indicate that the crustal remanent magnetic signature and density structure of the subsurface is very complex, reflecting either the original emplacement, or more likely subsequent modification.

Although the formation mechanism of the dichotomy is uncertain, it is agreed that it formed in the Noachian, creating a crustal thickness difference and likely a lithospheric thickness difference. The elevation and crustal thickness difference is capable of producing relaxation of the boundary for specific thermal and rheological conditions, producing deformation of the surface and subsurface parallel to the boundary (Guest and Smrekar, 2005). Relaxation may be responsible for formation of a topographic bench in the lowlands just north of the boundary, and various sets of faults that parallel the boundary in the Ismenius region (Smrekar et al., 2004). Faulting may influence the magnetic and density structures via hydrothermal alteration along faults, which can demagnetize or create magnetic minerals, and affect the density structure through serpentinization. Edge-driven convection, which may occur where there is a significant change in the lithospheric thickness, can create downwelling on the thin lithosphere side and upwelling on the thick side, potentially leading to long-term crustal thickness variations.

The wavelength of the Bouguer and isostatic gravity anomalies and magnetic anomalies in the plains adjacent to the dichotomy is typically several hundred kilometers, indicating that local scale processes are important. The one exception in our study region is the large positive density anomaly modeled by Kiefer (2005). Thus we infer that in most areas of the dichotomy boundary, igneous intrusion or crustal thinning/thickening are likely to have affected the thermal and density structure, perhaps initiated by Rayleigh–Taylor instabilities, or edge-driven convection. Kiefer (2005) rejects igneous intrusion based on the lack of observed volcanism. However, we note that Apollinaris Patera is located within approximately 250 km of the boundary, and that geologic mapping reveals numerous volcanic units (Tanaka et al., 1992, 2005). Hydrothermal alteration, if present on very large-scales, may also have contributed (Harrison and Grimm, 2002; Solomon et al., 2005) to density and magnetic contrasts within the crust.

6. Conclusions

The admittance signatures in our study areas, Amenthes and Aeolis, as well as in Ismenius (Smrekar et al., 2004), are relatively uniform along the dichotomy boundary. The low values of elastic thickness are consistent with the formation of the dichotomy in the Noachian, when heat flow was relatively high. The variations in loading signature, and especially the presence of top-loading, suggest that additional processes may have acted as loads on the lithosphere during the Noachian. There is abundant evidence that erosion and faulting have also modified the dichotomy, driven by mechanisms such as topographic relaxation (Guest and Smrekar, 2005; Nimmo, 2005) or possibly lithospheric flexure (Watters, 2003; Watters and

McGovern, 2006) or edge-driven convection (Smrekar et al., 2004; Kiefer, 2005). The bottom-loading signature for Amenthes may be due to the presence of a broad valley and may also influence the low elastic thickness estimates from crustal thinning. The top-loading in Aeolis may be related to surface volcanic deposits. The similarity in the wavelength and amplitude of the gravity and magnetic field anomalies and the constant ratio of the amplitudes of the anomalies along the dichotomy boundary imply that smaller scale processes have affected both the density and magnetization structure in our study area and in Ismenius (Smrekar et al., 2004). We conclude that igneous intrusion or crustal thinning/thickening are likely to have affected the thermal and density structure. If present on a large scale, hydrothermal alteration may also contribute. Future work will include detailed geologic studies of Amenthes and Aeolis, and 3D joint inversion of the gravity and magnetic fields as described in Milbury et al. (2005). Future work will use the magnetic field data from the AB and SPO, and MO phases of the Mars Global Surveyor mission as a tool to explore the differences in modeling results. Gravity data will be used to constrain the locations of the source bodies, due to the better spatial correspondence of the gravity anomalies and sources than the magnetic sources and anomalies. This may provide greater insight into processes creating gravity and magnetic anomalies, loading sources, and modification of the dichotomy.

Acknowledgments

This work was supported by NASA Graduate Student Research Program fellowship and a grant from the NASA Mars Data Analysis Program. We thank Christophe Sotin for his constructive review, which significantly improved the paper.

References

Albert, A., Phillips, R.J., 2000. Paleoflexure. Geophys. Res. Lett. 27 (16), 2385–2388.

Babeyko, A.Y., Zharkov, V.N., 2000. Martian crust: a modeling approach. Phys. Earth Planet. Interiors 117 (1-4), 421–435.

Banks, R.J., Parker, R.L., Huestis, S.P., 1977. Isostatic compensation on a continental scale: local versus regional mechanisms. Geophys. J. R. Astron. Soc. 51, 431–452.

Breuer, D., Yuen, D.A., Spohn, T., 1997. Phase transitions in the Martian mantle: implications for partially layered convection. Earth Planet. Sci. Lett. 148, 457–469.

Breuer, D., Yuen, D.A., Spohn, T., Zhang, S., 1998. Three-dimensional models of Martian mantle convection with phase transitions. Geophys. Res. Lett. 25, 229–232.

Burov, E.B., Diament, M., 1995. The effective elastic thickness (Te) of continental lithosphere: what does it really mean. J. Geophys. Res. 100 (B3), 3905–3928.

Connerney, J.E.P., Acuña, M.H., Wasilewski, P.J., Ness, N.F., Re'me, H., Mazelle, C., Vignes, D., Lin, R.P., Mitchell, D., Cloutier, P., 1999. Magnetic lineations in the ancient crust of Mars. Science 284, 794–798.

Connerney, J., Acuña, M.H., Wasilewski, P.J., Kletetschka, G., Ness, N.F., Re'me, L.R.P., Mitchell, D., 2001. The global magnetic field of Mars and implications for crustal evolution. Geophys. Res. Lett. 28 (21), 4015–4018.

Dorman, L.M., Lewis, B.T.R., 1970. Experimental isostasy, I: Theory of the determination of the earth's isostatic response to a concentrated load (1970). J. Geophys. Res. 75, 3357–3365.

Forsyth, D.W., 1985. Subsurface loading and estimates of the flexural rigidity of continental lithosphere. J. Geophys. Res. 90, 12623.

Frey, H.V., 2006. Impact constraints on the age and origin of the lowlands of Mars, Geophys. Res. Lett. 33, L08S02, doi:10.1029/2005GL024484.

Frey, H.V., Schultz, R.A., 1988. Large impact basins and the mega-impact origin for the crustal dichotomy. Geophys. Res. Lett. 15, 229–232.

Frey, H.V., Roark, J.H., Shockey, K.M., Frey, E.L., Sakimoto, S.E.H., 2002. Ancient lowlands on Mars. Geophys. Res. Lett. 29 (10).

Guest, A., Smrekar, S.E., 2005. Relaxation of the Martian dichotomy boundary: faulting in the Ismenius region and constraints on the early evolution of Mars. J. Geophys. Res. 110, E12S25.

Harrison, K.P., Grimm, R.E., 2002. Controls on Martian hydrothermal systems: application to valley network and magnetic anomaly formation. J. Geophys. Res. 107, 5025.

Hoogenboom, T., Smrekar, S.E., 2006. Elastic thickness estimates for the northern lowlands of Mars, submitted.

Kiefer, W.S., 2005. Buried mass anomalies along the hemispheric dichotomy in eastern Mars: implications for the origin and evolution of the dichotomy. Geophys. Res. Lett. 32, L22201.

Langlais, B., Purucker, M.E., Mandea, M., 2004. Crustal magnetic field of Mars. J. Geophys. Res. 109, E02008.

McGovern, P.J., et al., 2002. Localized gravity/topography admittance and correlation spectra on Mars: implications for regional and global evolution. J Geophys. Res. 107 (E12), 5136.

McGill, G.E., Dimitriou, A.M., 1990. Origin of the Martian global dichotomy by crustal thinning in the late Noachian or early Hesperian. J. Geophys. Res. 95, 12595–12605.

McKenzie, D., Barnett, D.N., Yuan, D., 2002. The relationship between Martian gravity and topography. Earth Planet. Sci. Lett. 195, 1–16.

McNutt, M.K., 1983. Influence of plate subduction on isostatic compensation in northern California. Tectonics 2, 399–415.

Milbury, C.A., Raymond, C.A., Jewell, J.B., Smrekar, S.E., Schubert, G., 2005. Joint inversion and forward modeling of gravity and magnetic data in the Ismenius region of Mars. Lunar Planet. Sci. [CD-ROM], XXXVI, abstract 2075.

Neumann, G.A., Zuber, M.T., Wieczorek, M.A., McGovern, P.J., Lemoine, F.G., Smith, D.E., 2004. Crustal structure of Mars from gravity and topography. J. Geophys. Res. 109, E08002.

Nimmo, F., 2002. Admittance estimates of mean crustal thickness and density at the Martian hemispheric dichotomy. J. Geophys. Res. 107 (E11), 5117.

Nimmo, F., 2005. Tectonic consequences of Martian dichotomy modification by lower crustal flow and erosion. Geology 33, 533–536.

Perez-Gussinye, M., Lowry, A.R., Watts, A.B., Velicogna, I., 2004. On the recovery of effective elastic thickness using spectral methods: examples from synthetic data and from the Fennoscandian Shield. J. Geophys. Res. 109 (B10409).

Petit, C., Ebinger, C., 2000. Flexure and mechanical behavior of cratonic lithosphere: gravity models of the East African and Baikal rifts. J. Geophys. Res. 105 (B8), 19151–19162.

Phillips, R.J., et al., 2001. Ancient geodynamics and global-scale hydrology on Mars. Science 291, 2587–2591.

Schubert, G., Lingenfelter, R.E., 1973. Martian centre of mass-centre of figure offset. Nature 242, 251–252.

Simons, F.J., Zuber, M.T., Korenaga, J., 2000. Isostatic response of the Australian lithosphere: estimation of effective elastic thickness and anisotropy using multitaper spectral analysis. J. Geophys. Res. 105, 19163–19184.

Sleep, N.H., 1994. Martian plate tectonics. J. Geophys. Res. 99, 5639–5655.

Smrekar, S.E., McGill, G.E., Raymond, C.A., Dimitriou, A.M., 2004. Geologic evolution of the Martian dichotomy in the Ismenius area of

Mars and implications for plains magnetization. J. Geophys. Res. 109, E11002.
Solomon, S.C., et al., 2005. New perspectives on ancient Mars. Science 307, 1214–1220.
Swain, C.J., Kirby, J.K., 2003. The effect of 'noise' on estimates of elastic thickness of the continental lithosphere by the coherence method. Geophys. Res. Lett. 30, 11.
Tanaka, K.L., Scott, D.H., Greeley, R., 1992. Global stratigraphy. In: Kieffer, H.H., et al. (Eds.), Mars. Univ. Ariz. Press, Tucson, pp. 345–382.
Tanaka, K.L., Skinner, J.A., Hare, T.M., 2005. Geologic Map of the Northern Plains of Mars. Scientific Investigations Map 2888, U.S. Geological Survey, Reston, VA, 1:15M.
Turcotte, D.L., Shcherbakov, R., Malamud, B.D., Kucinskas, A.B., 2002. Is the Martian crust also the Martian elastic lithosphere. J. Geophys. Res. 107 (E11), 5091.
Watters, T.R., 2003. Lithospheric flexure and the origin of the dichotomy boundary on Mars. Geology 31, 271–274.
Watters, T.R., McGovern, P.J., 2006. Lithospheric flexure and the evolution of the dichotomy boundary on Mars. Geophys. Res. Lett. 33, L08S05.
Watts, A.B., Zhong, S., 2000. Observations of flexure and the rheology of oceanic lithosphere. Geophys. J. Int. 142.
Wieczorek, M.A., Simons, F.J., 2005. Localized spectral analysis on the sphere. Geophys. J. Int. 162, 99.
Wilhelms, D.E., Squyres, S.W., 1984. The Martian hemispheric dichotomy may be due to a giant impact. Nature 309, 138–140.
Wise, D.U., Golombek, M.P., McGill, G.E., 1979a. Tharsis province of Mars: geologic sequence, geometry, and a deformation mechanism. Icarus 38, 456–472.
Wise, D.U., Golombek, M.P., McGill, G.E., 1979b. Tectonic evolution of Mars. J. Geophys. Res. 84, 7934–7939.
Yuan, D., Sjogren, W., Konopliv, A., Kucinskas, A., 2001. Gravity field of Mars: a 75th Degree and Order Model. J. Geophys. Res. 106 (E10), 23377–23402.
Zhong, S., Zuber, M.T., 2001. Degree-1 mantle convection and the crustal dichotomy on Mars. Earth Planet. Sci. Lett. 189, 75–84.
Zuber, M.T., 2001. The crust and mantle of Mars. Nature 412, 220–227.
Zuber, M.T., et al., 2000. Internal structure and early thermal evolution of Mars from Mars Global Surveyor topography and gravity. Science 287, 1788–1793.